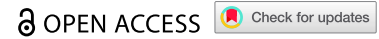


RESEARCH ARTICLE



# Enhancing recovery from gut microbiome dysbiosis and alleviating DSS-induced colitis in mice with a consortium of rare short-chain fatty acid-producing bacteria

Achuthan Ambat<sup>a,b,\*</sup>, Linto Antony<sup>a,\*</sup>, Abhijit Maji<sup>a</sup>, Sudeep Ghimire<sup>a</sup>, Samara Mattiello<sup>a</sup>, Purna C. Kashyap<sup>c</sup>, Sunil More<sup>b</sup>, Vanessa Sebastian<sup>d</sup>, and Joy Scaria<sup>a,b</sup>

<sup>a</sup>Department of Veterinary and Biomedical Sciences, South Dakota State University, Brookings, SD, USA; <sup>b</sup>Department of Veterinary Pathobiology, College of Veterinary Medicine, Oklahoma State University, Stillwater, OK, USA; <sup>c</sup>Enteric Neuroscience Program, Department of Medicine and Physiology, Mayo Clinic, Rochester, MN, USA; <sup>d</sup>Department of Pathology, Jubilee Mission Medical College and Research Institute, Thrissur, India

## ABSTRACT

The human gut microbiota is a complex community comprising hundreds of species, with a few present in high abundance and the vast majority in low abundance. The biological functions and effects of these low-abundant species on their hosts are not yet fully understood. In this study, we assembled a bacterial consortium (SC-4) consisting of *B. paravirosa*, *C. comes*, *M. indica*, and *A. butyriciproducens*, which are low-abundant, short-chain fatty acid (SCFA)-producing bacteria isolated from healthy human gut, and tested its effect on host health using germ-free and human microbiota-associated colitis mouse models. The selection also favored these four bacteria being reduced in abundance in either Ulcerative Colitis (UC) or Crohn's disease (CD) metagenome samples. Our findings demonstrate that SC-4 can colonize germ-free (GF) mice, increasing mucin thickness by activating MUC-1 and MUC-2 genes, thereby protecting GF mice from Dextran Sodium Sulfate (DSS)-induced colitis. Moreover, SC-4 aided in the recovery of human microbiota-associated mice from DSS-induced colitis, and intriguingly, its administration enhanced the alpha diversity of the gut microbiome, shifting the community composition closer to control levels. The results showed enhanced phenotypes across all measures when the mice were supplemented with inulin as a dietary fiber source alongside SC-4 administration. We also showed a functional redundancy existing in the gut microbiome, resulting in the low abundant SCFA producers acting as a form of insurance, which in turn accelerates recovery from the dysbiotic state upon the administration of SC-4. SC-4 colonization also upregulated iNOS gene expression, further supporting its ability to produce an increasing number of goblet cells. Collectively, our results provide evidence that low-abundant SCFA-producing species in the gut may offer a novel therapeutic approach to IBD.

## ARTICLE HISTORY

Received 12 September 2023  
Revised 24 May 2024  
Accepted 16 July 2024

## KEYWORDS



Microbiome; colitis; short chain fatty acid; butyrate; low abundant species; defined bacterial therapy; insurance species

## Introduction


In biological ecosystems, species composition typically follows a skewed pattern, wherein a small subset of species is highly abundant, whereas the majority are low in abundance or relatively rare. This phenomenon, first observed by Darwin in his groundbreaking work,<sup>1</sup> is a common characteristic across diverse biological classes and geographies. The same skewed distribution was later recognized by Preston in bird and moth populations during the 20th century.<sup>2</sup> This skewed biodiversity distribution is also reflected in the composition of the human gut microbiota. An analysis of the gut microbiome composition of individuals across various continents revealed a bimodal species

distribution.<sup>3</sup> In this distribution, a handful of highly abundant species exist on the left of the log-normal distribution, whereas a large number of rare species congregate on the right. Upon further exploration of species distribution across thousands of individuals, Lawley et al. discovered that the human gut microbiota is primarily dominated by approximately 20 species, with the remaining species present in lower abundances.<sup>4</sup>

Therefore, the focus of human gut microbiome research has been primarily directed toward understanding the roles and implications of these dominant species. Numerous studies have found that these highly abundant species often play vital roles

**CONTACT** Joy Scaria  [joy.scaria@okstate.edu](mailto:joy.scaria@okstate.edu)  Department of Veterinary Pathobiology, College of Veterinary Medicine, Oklahoma State University, Venture One Building, 1110 S Innovation Dr, Stillwater, OK 74074, USA

\*Equally contributing authors.

 Supplemental data for this article can be accessed online at <https://doi.org/10.1080/19490976.2024.2382324>

© 2024 The Author(s). Published with license by Taylor & Francis Group, LLC.

This is an Open Access article distributed under the terms of the Creative Commons Attribution License (<http://creativecommons.org/licenses/by/4.0/>), which permits unrestricted use, distribution, and reproduction in any medium, provided the original work is properly cited. The terms on which this article has been published allow the posting of the Accepted Manuscript in a repository by the author(s) or with their consent.

in gut functionality. One such species is *Bacteroides thetaiotaomicron*, which is a common inhabitant of the human gut. Extensive research on this organism has provided valuable insights into how dominant members of the microbiome contribute to maintaining health and well-being. *B. thetaiotaomicron* plays a key role in nutrient utilization in the gut, where it helps metabolize polysaccharides that are otherwise inaccessible to the host.<sup>5</sup> Another well-understood example of a highly abundant gut species is *Faecalibacterium prausnitzii*, which has been recognized as one of the main butyrate producers in the intestine.<sup>6</sup> The presence of highly abundant species can also be problematic. A well-known example for that is *Escherichia coli* which depending on the strain type could proliferate in the dysbiotic gut can cause mild to fulminant diarrhea.<sup>7</sup>

Metagenomic investigations of the gut microbiome have revealed several thousand species spanning diverse populations, with the majority being identified as low-abundance species. Intriguingly, most of these rare species have not been cultured, and even among them, comprehensive functional and mechanistic studies are sparse. Despite possessing a reasonable understanding of certain dominant species residing in the gut, our knowledge of the role of these rare species remains largely underexplored. However, emerging research indicates that these low-abundance species may profoundly influence host health and serve as potent activators of gut immunity among other potential effects. Eventually, these species contribute to the total richness and diversity of the system. In contrast, loss of diversity has been associated with various enteric and systemic diseases,<sup>8</sup> further suggesting that these species might play a significant role in protection against these diseases.

In non-microbial communities, higher rates of extinction have motivated interest in diversity–stability relationships.<sup>9–12</sup> The insurance hypothesis states that high species richness reduces the temporal variability of a given community property by insuring the community against various perturbations.<sup>13</sup> The same concept has been observed in microbial communities. For example, Lieven et al. showed in experimental microcosms that the degree of richness and evenness in a community prior to perturbation affects the subsequent response.<sup>14</sup> Later, the same was explained for conditionally rare taxa (CRT) in the gut microbiome.<sup>15</sup>

The objective of our study was to delve deeper into the functional roles of rare species in the gut, particularly those capable of producing short-chain fatty acids (SCFAs). SCFAs were selected as the focal point because of their significant contributions to immune cell proliferation,<sup>16</sup> differentiation,<sup>17</sup> apoptosis,<sup>18</sup> gut barrier integrity,<sup>19</sup> gut motility,<sup>20</sup> and host metabolism.<sup>21</sup> Among the characterized SCFAs, butyrate has demonstrated protective effects against immune disorders such as Inflammatory Bowel Disorder (IBD).<sup>22</sup> Although the direct administration of butyrate compounds as a therapeutic intervention against IBD has encountered obstacles related to delivery, exposure duration, and patient compliance, there is continued interest in the beneficial properties of butyrate.<sup>23,24</sup> The success of using prebiotics for IBD treatment depends on the presence of butyrate-producing bacteria.<sup>25</sup> For instance, treatment with butyrate-producing *F. prausnitzii* was found to restore the aberrant microbiota community in an IBD mouse model, whereas *Butyricicoccus pullicaecorum* attenuated colitis in rats.<sup>26</sup> Given the scarcity of functional studies on rare gut species, we employed germ-free (GF) and humanized mouse models to explore the interspecies interactions of a manageable consortium of four SCFA-producing rare species in the human gut. We reasoned the selection of the strains based on the lower abundance in healthy metagenome, presence in the previously formulated culture library, ability to produce SCFA specifically butyrate and its differential abundance in IBD metagenome samples. We also utilized dietary fibers as supplements in humanized mice experiment to increase the abundance of these SCFA-producing bacterial members, thereby expecting to see an improvement in disease outcomes. Our findings indicated that the rare species mix we utilized colonized GF mice and alleviated DSS-induced colitis. In humanized mice, the same mix expedited the recovery of microbiome beta diversity and enhanced host health following Dextran Sodium Sulfate (DSS) perturbation. Our study also demonstrates the existence of functional redundancy within the gut microbiome, where low-abundant short-chain fatty acid (SCFA) producers playing a crucial role as a resilience factor. This redundancy facilitates a faster recovery from

dysbiotic states upon the administration of SC-4. The colonization by SC-4 not only accelerates recovery but also upregulates the expression of the iNOS gene, contributing to an increase in mucin producing goblet cells. Taken together, our findings suggest that enhancing the population of low-abundant SCFA-producing bacteria in the gut may represent a new therapeutic strategy for managing IBD.

## Results

### Selection of strains for short chain fatty acid producing consortium (SC-4)

In our previous study, we developed a microbiota culture collection from healthy human donors that accounted for over 70% of the functional capacity of the healthy gut microbiome.<sup>27</sup> This collection included both high and rare abundant species. To curate a collection of short-chain fatty acid (SCFA)-producing strains from our library, we focused on several criteria: their ability to produce SCFAs, their low abundance nature, and their

differential abundance in disease datasets. Given the association of butyrate with inflammatory bowel disease (IBD), our selection was particularly guided by the strains' capacity to produce butyrate. This determination was based on both experimental inference and existing literature. Recognizing that the genes responsible for butyrate production in bacteria are well-documented, we primarily used the presence of these genes as the criterion for species selection in our study.

First, we determined the percentage abundance of already reported butyrate-producing bacteria in the donor fecal samples used for developing our culture collection<sup>27</sup> (Figure 1(a)) as well as in a publicly available healthy human shotgun metagenomics dataset<sup>28</sup> (Figure 1(b)).<sup>27,29–32</sup> Consistent with prior reports, our analysis revealed that the well-known butyrate-producing species *F. prausnitzii* was highly abundant in donor metagenomes. Nevertheless, the mean abundance of most putative butyrate-producing species was less than 0.1%. To constitute a manageable mix of strains for further study, we randomly selected four species with abundances below this threshold

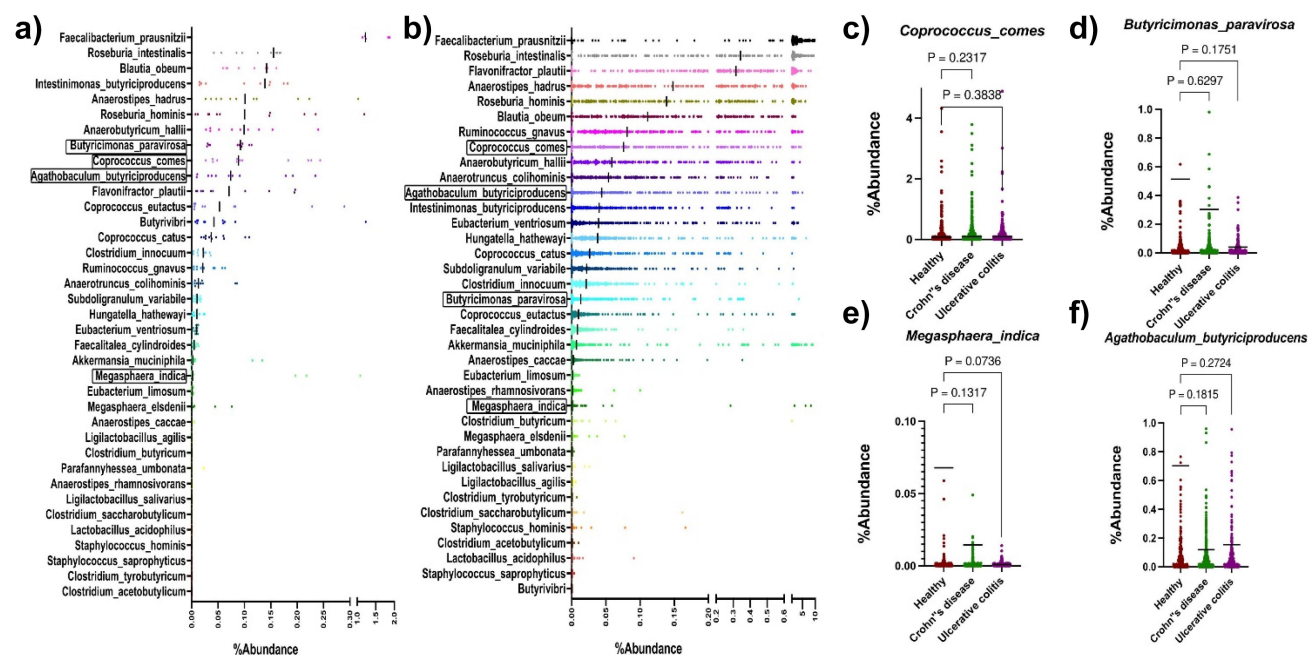


**Figure 1.** Butyrate-synthesizing bacteria primarily belong to the low dominant category of the human gut. Percentage abundance of Butyrate-producing bacteria in Donor (a) and healthy people fecal metagenome samples from a previously published study<sup>59</sup> (b). The highlighted species outlined in box are included in the SC-4 consortia and the dark black line for each species represents the median percentage abundance. The abundance of *Coproccoccus comes* (c), *Butyricimonas paravirosa* (d), *Megasphaera indica* (e), and *Agathobaculum butyriciproducens* (f) in UC, CD patient, and healthy people sample from a previously published study.<sup>28</sup> Comparisons between groups were performed using either the Mann–Whitney *t*-test. Absolute *p*-value is represented in the graphs.

(Supplementary Figure S1a). The abundance of these selected strains, measured from the metagenome sequence data of six donor fecal samples, showed that all four bacteria exhibited a mean abundance of less than 0.1% (Figure 1(a,b), Supplementary Figure S1a & b).

The relative abundance of the presumptive butyrate-producing species in our dataset was aligned with the relative distribution across the analyzed public datasets (Figure 1(b-f)). The genotypic and phenotypic potential of the selected strains to produce butyrate served as the criteria for their selection. To confirm their genotypic potential, their genome sequences<sup>27</sup> were scrutinized using BLAST to identify markers of the butyrate synthesis pathway, specifically butyryl-CoA: acetate CoA transferase (encoded by *but*) or butyrate kinase (encoded by *buk*). These two genes represent terminal genes in the most prevalent pathway of butyrate production in the gut microbiota.<sup>33</sup> *Butyricimonas paravirosa* and *Coprococcus comes* exhibited the presence of *but*, whereas *Megasphaera indica* and *Agathobaculum butyriciproducens* demonstrated the presence of *buk* in their genome (Supplementary Figure S1c). Their ability to produce butyrate and other SCFAs was confirmed by *in vitro* culture of the strains in three different media, followed by gas chromatography estimation of SCFAs in the culture supernatant (Supplementary Figure S1d).

Depletion or enrichment of a bacterial species in a disease condition might indicate the role of that bacterial species in the prevention or exacerbation of the disease, respectively. Nonetheless, this association does not prove their causal relationship with the disease. Thus, to determine the association of selected species with IBD, a disease prevalent in both developed and developing countries,<sup>34</sup> the abundance of these bacteria was assessed in fecal metagenomes collected from IBD and non-IBD individuals as part of a longitudinal cohort study conducted by Lloyd-Price et al.<sup>28</sup> We assessed the abundance of all four species in 598 metagenomes from 50 Crohn's Disease (CD) subjects and 375 metagenomes from 30 Ulcerative Colitis (UC) subjects. We compared it against the abundances of 365 metagenomes from 27 non-IBD subjects. Interestingly, the analysis showed the presence of all four bacterial families under both conditions

(healthy and diseased) with a mean abundance of <0.1% (Figure 1(c-f)). Compared to the non-IBD microbiota, all four bacteria showed differential abundances in at least one of the IBD conditions. The median abundance of *Agathobaculum butyriciproducens*, *Megasphaera indica*, and *Butyricimonas paravirosa* was decreased in both UC and CD patients (Figure 1d-f). We did not find an appealing difference in the median abundance of *Coprococcus comes* in either patients with UC or CD patients. We believe that the lack of statistical confidence is due to the increase in sample size and low abundant nature of the species itself. These results confirmed that there is a reduction in the number of SC-4 bacteria in the gut of IBD patients, indirectly pointing to the fact that SC-4 bacteria have a negative correlation with IBD condition. Altogether, the selected species represented low abundant SCFA producing bacteria shown differential abundance in disease datasets.

#### **Estimation of intra-consortium interaction of SC-4 in vivo**

One hypothesis for species being rare within a community is competition with other species. To assess whether the chosen rare species could stably colonize the host gut and to investigate the interactions between these low-abundance species, we employed a germ-free mouse model to polysociate the SC-4 consortium. After administering equal proportions of the SC-4 mix orally via gavage, fecal samples were collected at different time points to assess the bacterial load. An average bacterial load of  $>10^7$  CFU/g feces was detected from the 4th day post-inoculation (DPI), which continued to increase until it reached  $>10^8$  CFU/g feces (Supplementary Figure S2a). During these time points, we did not observe any significant drop in the bacterial load, suggesting successful and stable colonization of the SC-4 consortium in the mouse gut. An average bacterial count of nearly  $10^9$  CFU/g in the cecal content (Supplementary Figure S2) further verified the successful colonization of these allochthonous host species.

Community profiling via 16s rRNA gene amplicon sequencing revealed the presence of all four bacteria, although their abundance varied and

remained consistent throughout the experiment (Figure 2(a), Supplementary Figure S2c-e). We found a similar community structure in the cecum and colon, but we did not obtain any amplification for 16s PCR from the small intestine contents (Figure 2(a), Supplementary Figure S2c). This demonstrated the ability of the consortium to colonize the distal gut of germ-free mice. *C. comes* had a higher mean abundance in all mice, whereas *A. butyriciproducens*, *B. paraviroso*, and *M. indica* displayed relatively lower abundance in colonized mice. Next, we examined whether the colonized consortium could produce butyrate and other short-chain fatty acids (SCFAs). As anticipated, the colonized consortium was capable of producing butyrate and other SCFAs. Analysis of cecal

content using gas chromatography (GC) detected significantly higher levels of all key SCFAs, except acetate, in SC-4 colonized mice compared to germ-free mice (Figure 2(b)).

### Colonization of SC-4 modulates the host immune system

To explore how the consortium interacted with the host, we analyzed the expression profile of a panel of 91 genes in the colon using quantitative real-time PCR (qRT-PCR). When compared to germ-free (GF) mice, nine genes showed more than a two-fold change in their expression in the SC-4 colonized group (Figure 2(c)). Colonizing GF mice with a potential pathogen usually increases the

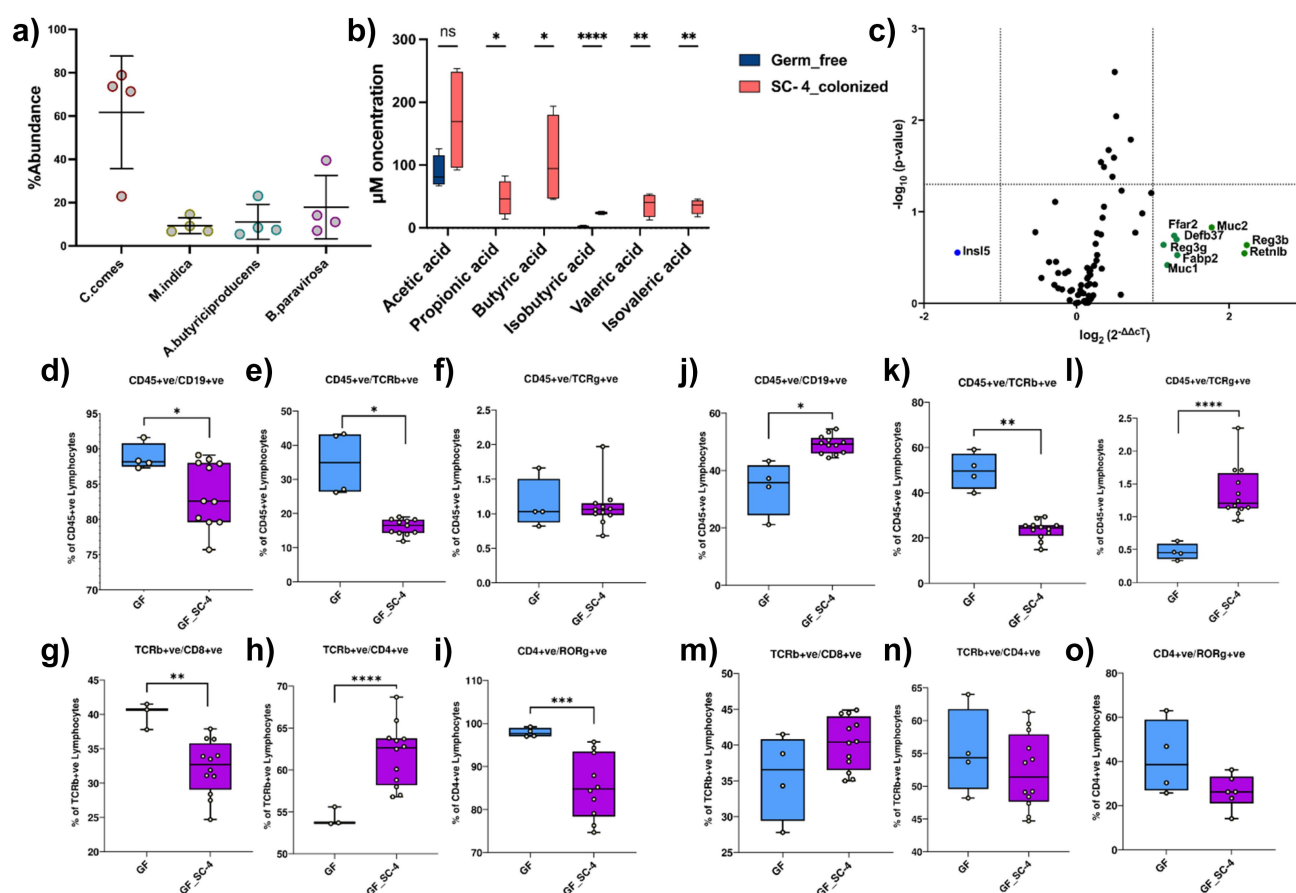


**Figure 2.** SC-4 successfully colonized germ-free mice. Percentage abundance of *Coprococcus comes*, *Butyricimonas paraviroso*, *Megasphaera indica*, and *Agathobaculum butyriciproducens* (a), and box plot representing concentration of SCFAs in mice cecum colonized with SC-4 (b). RT-PCR gene expression for Rt2 profiler array consisting of 88 genes of mice colon, colonized with SC-4 (c). Green dots – overexpressed more than twofold change, blue dots – repress more than twofold compared to GF control (dotted lines on the x-axis represent a twofold increase or decrease in expression and the y-axis represent a  $p$ -value cutoff of .05). Percentage cell population of lymphocytes in the spleen of GF and GF colonized with SC-4 mice (d-i). Comparisons between groups were performed using either the Mann–Whitney  $U$ -test or the  $t$ -test with Welch's correction. Significance levels were indicated as follows: ns for not-significant, \* for  $p$ -values < .05, \*\* for  $p$ -values < .01, and \*\*\* for  $p$ -values < .001.

expression of various pro-inflammatory and anti-inflammatory cytokines, as well as Toll-Like Receptors (TLRs), in the intestine<sup>35</sup>. The absence of significant changes in the expression levels of these genes and intestinal barrier proteins in the colon suggests that the SC-4 species do not negatively impact the host, even when colonized at high levels. Notably, changes in expression were found primarily in genes involved in the host's initial immune defenses, including mucins (MUC-1 and MUC-2) and antimicrobial peptides (Reg3b, Reg3g, Retnlb, and Defb37). Interestingly, SC-4 colonization also increased the expression of fatty acid-binding protein 2 (FABP2/I-FABP) and one of the G-protein coupled receptors (GPRs), FFAR2, or GPR43 (Figure 2(c)). FABP2 is a cytosolic protein that binds to Free Fatty Acids (FFA) and is thought to be involved in the uptake and intracellular trafficking of lipids in the intestine. Conversely, FFAR2 is a receptor for short-chain fatty acids.<sup>36</sup> We believe that since the colonized members of SC-4 are capable of producing butyrate in the mouse gut, and butyrate is an energy source for colonocytes, the expression of insulin-like peptide 5 (Insl5) showed more than two-fold downregulation.

To better understand the adaptive immune changes elicited by the colonization of SC-4, we profiled total lymphocytes (CD45+) collected from both secondary lymphoid organs (spleen) and peripheral blood. Flow cytometry analysis of major adaptive immune cell populations, such as B-cells (CD19+), bd-T cells, and subsets of ab-T cells – T-helper (CD4+), T-cytotoxic (CD8+), and Th17 (RORγ+) – showed noticeable differences in the adaptive immune phenotypes between GF and SC-4 colonized mice. Interestingly, the percentage of B cells and ab-T cells in the total lymphocytes was significantly lower in the spleen of SC-4 colonized mice (Figure 2(d-f)). Within ab-T cells, there was a significant decrease in CD8+ T cells and increase in CD4+ T cells (Figure 2g,h). However, the percentage of Th17 cells among CD4+ T cells was significantly reduced in GF mice (Figure 2(i)).

In the peripheral blood, ab-T cells showed a similar trend as in the spleen, but there were no significant differences in the proportions of CD4+, CD8+, and Th17 cells compared to GF mice. However, Th17 cells showed a decrease in the

proportion of CD4+ T cells, although the difference was not statistically significant (Figure 2(n)). In contrast to the spleen, B cells and bd-T cells were significantly increased in BP4 colonized mice (Figure 2(d-o)). Histopathological analysis of colon tissue after H&E staining showed normal appearance in both GF- and BPC-colonized gnotobiotic mice without any disruption in mucosal architecture (Supplementary Figure S3d). However, some morphological changes were observed between the two groups. Both villus length and crypt depth were increased in gnotobiotic mice than in the GF controls. The submucosa and muscularis propria were thicker in gnotobiotic mice than in GF mice but without any pathological signs such as submucosal edema. We believe this could be related to the increase in expression of MUC-1 and MUC-2 genes when GF mice were colonized with the SC-4 consortium.

#### ***SC-4 colonization protects GF mice from DSS-induced colitis***

As the colonization of SC-4 induced positive immune changes in GF mice, we further examined whether this modulation could provide protection against disorders such as IBD. To determine this, SC-4 pre-colonized mice were treated with DSS to induce colitis and monitored throughout the experiment and the mice were sacrificed on day 21 (Supplementary Figure S3a). The communities formed in the colon and cecum were assessed using 16s rRNA sequencing along with disease status determination using histology assessment of colon samples. Colitis in mice is often characterized by noticeable changes such as shortening of the colon. Interestingly, our results showed that SC-4 pre-colonized mice exhibited less colon shrinkage than the control group (Figure 3(a,b)), suggesting that SC-4 pre-colonization may offer systemic protection against DSS-induced colitis. SC-4 colonization also protected mice against colitis-induced death (Supplementary Figure S3b). Histopathological analysis of GF mice with colitis showed moderate inflammation, loss of goblet cells, vascular proliferation, and wall thickening; however, mice pretreated with SC-4 showed no to mild inflammation in most samples as indicated by the decrease in pathology score (Figure 3c,

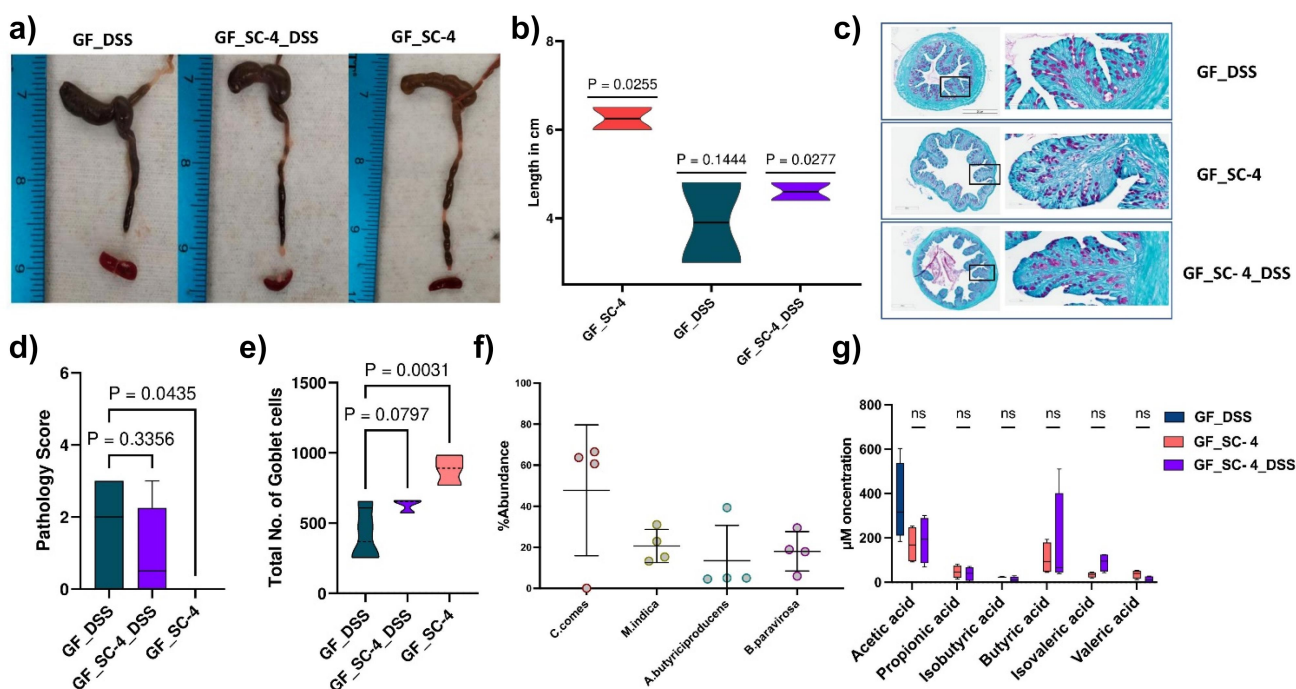


**Figure 3.** SC-4 confers protection against DSS-induced colitis. Representative colon from germ-free (GF) mice induced with colitis (GF\_DSS), GF mice gavaged with SC-4 bacteria (GF\_SC-4) and GF mice gavaged with SC-4 bacteria induced with colitis (GF\_SC-4\_DSS) (a) and associated violin plot (b) representing the length of the colon in cm. Statistical significance is calculated using one sample *t*-test across the complete population and the absolute value for each group is represented above each violin plot. Representative histopathological photograph showing the colon tissue cross-section after PAS staining GF\_DSS, GF\_SC-4 and GF\_SC-4\_DSS mice groups (c). Box plot mentioning the pathology score calculated from the histopathological section of colon tissue cross section after H&E staining as mentioned in (Supplementary Figure S3D) (d). Truncated violin plot representing total number of goblet cells counted from the histopathological section of colon tissue cross section after PAS staining as mentioned in (c) (e). Statistical significance for D & E calculated using one-way ANOVA with Dunnett correction with absolute *p*-value represented on the graph. Percentage abundance of SC-4 bacteria (f) and box plot representing concentration of SCFAs (g) in mice cecum upon DSS treatment. Comparisons between groups were performed using either the Mann–Whitney *U*-test or the *t*-test with Welch’s correction.

Supplementary Figure S3c). Since we did identify substantial differences in MUC-1 and MUC-2 gene upon SC-4 colonization, we hypothesized that the protective effect conferred by SC-4 might be attributed to the improvement of gut barrier function. These genes, which contribute to the thickness of the submucosa and muscularis propria, may enhance barrier function. PAS staining on the histology sections showed a significant increase in the number of goblet cells present confirming the hypothesis (Figure 3(c,e)). The 16s rRNA sequencing of the feces showed the same trend as that previously observed for SC-4 colonization (Figure 3(f)). *C. comes* relative abundance slightly decreased with an increase in abundance for the rest of the three species (Figure 3(f)). This suggests that *C. comes* may have an antagonistic effect on the other three species. This trend remained true for both the samples taken from colon and the

cecum (Figure 3(f), Supplementary Figure S3c). Furthermore, quantification of short-chain fatty acids showed no difference when treated with DSS (Figure 3g). A slight increase in butyrate production was also observed. This implies that the induction of a disease state does not reduce SC-4 ability to produce SCFAs.

Furthermore, we examined the differential gene expression upon disease induction for selected genes from the previous panel (Figure 2(c), Supplementary Table S1). However, compared with the control, SC-4 mice treated with DSS did not show any biologically relevant changes (Figure 4(a,b)). We also checked for the systemic immune response; apart from ab-T cells, there were no significant changes in the cell profile in DSS-treated animals (Figure 4(c–n)). There was a substantial reduction in the ab-T cell population in both PBMC and spleen of SC-4 pre-colonized

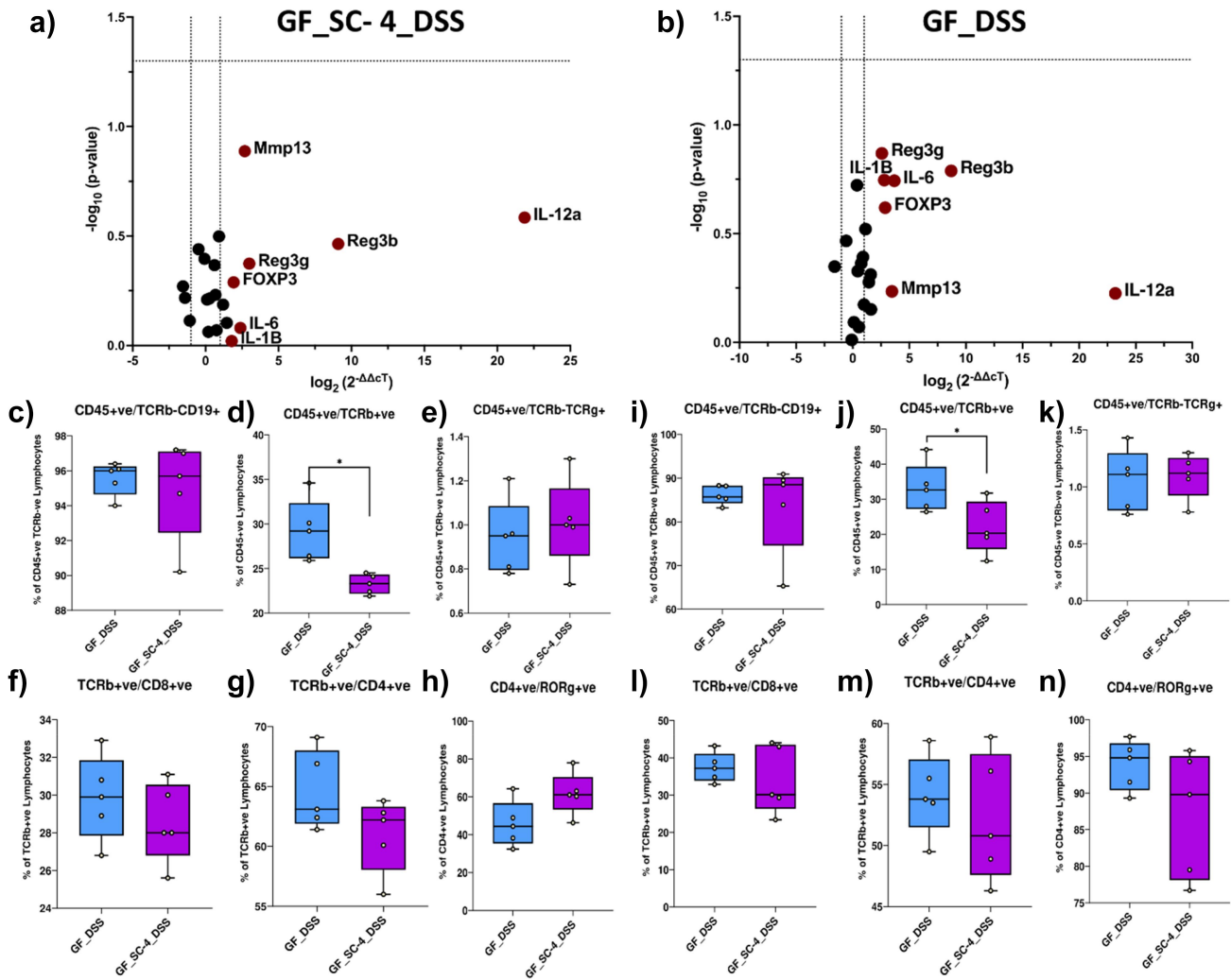


**Figure 4.** Local and systemic immune response in colitis model of GF mice treated with SC-4. RT-PCR gene expression for selected 25 immune-related genes of mice colon, GF mice pre colonized with SC-4 and then induced with colitis (GF\_SC-4\_DSS) (a) and GF mice induced with colitis (GF\_DSS) compared to GF control (b). Green dots – overexpressed more than twofold change, Red dots – overexpressed more than twofold compared to GF control (dotted lines on the x-axis represent a twofold increase or decrease in expression and the y-axis represent a  $p$ -value cutoff of .05). The percentage cell population of lymphocytes in the spleen of GF and GF colonized with SC-4 induced with colitis (c-h). The percentage cell population of lymphocytes in the spleen of GF and GF colonized with SC-4 mice induced with colitis (i-n). Comparisons between groups were performed using either the Mann–Whitney  $U$ -test or the  $t$ -test with Welch’s correction. Significance levels were indicated as follows: \* for  $p$ -values < .05, \*\* for  $p$ -values < .01, and \*\*\* for  $p$ -values < .001.

mice (Figure 4(d,j)). This result is comparable to that previously observed when GF mice were colonized with SC-4 (Figure 3(j,m)). However, no significant TH17 cells were increased in the spleen nor PBMC of GF mice with colitis. Our assumption for this change could be attributed to the previous recognition of the molecular patterns of the SC-4 consortium. Taken together, SC-4 consortium protect against DSS induced colitis in GF mice by improving the mucus barrier function.

#### **SC-4 members show a negative correlation with colitis in humanized mice**

Next, we examined whether the SC-4 consortium could colonize mice, establish a higher abundance, modulate microbiome composition, and improve host health in the presence of complex human microbiota. To this end, we gavaged the SC-4 consortium in human fecal microbiota-colonized mice. The composition of the microbiome following SC-4 gavage was analyzed by 16s rRNA

sequencing of the fecal pellets. While *Butyricimonas paravirosa* (Odoribacteraceae), *Coprococcus comes* (Lachnospiraceae) and *Agathobaculum butyriciproducens* (Ruminococcaceae) were detected in the community (Figure 5(a,h)), *Megasphaera indica* (Veillonellaceae) was not detected in any of the mice. This indicates that these three bacteria can colonize the mouse gut, even when introduced as part of a complex community. Furthermore, we examined whether the abundance of these three species changes during colitis. To this end, we induced colitis in SC-4 colonized humanized mice. The abundance of all three species was significantly reduced on the 6th day post-induction (Figure 5(a)). However, the reduction in abundance reverted significantly on the 28th day post-gavage when the mice started to recover from colitis (Figure 5(a)). This indicated a negative

correlation between these three species and colitis in mice. As the abundance of these bacteria increased with time post-gavage, we hypothesized that the introduction of these species back into the system could help accelerate recovery from DSS-induced colitis (Supplementary Figure S4a).

We examined the microbiome composition following these experiments and found that the introduction of SC-4 increased the alpha diversity of the gut community in DSS-treated mice, whereas it was lower in control mice (Figure 5(b), Supplementary Figure S5a-d). When the beta diversity between the different groups was examined, we observed that SC-4 administration after colitis induction shifted the diversity to resemble that of healthy humanized mice (Figure 5b, Supplementary Figure S5e-h). This suggests that introducing SC-4 can increase diversity and shift the microbiome to a controlled state. Besides the

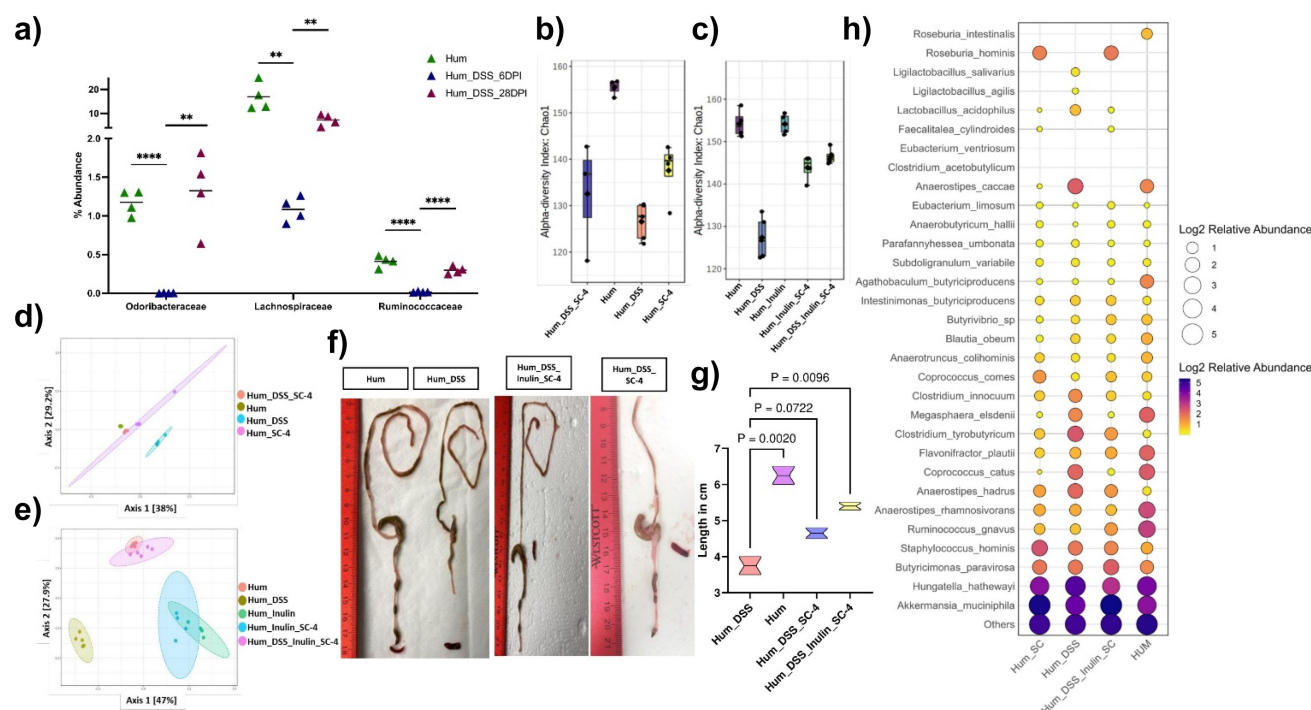


**Figure 5.** SC-4 colonization increases microbiome diversity. Percentage abundance of *Butyricimonas paravirosa* (Odoribacteraceae), *Coprococcus comes* (Lachnospiraceae), or *Agathobaculum butyriciproducens* (Ruminococcaceae) in humanized mice (Hum), humanized mice induced with colitis (Hum\_DSS) at 6th and 28th day post-infection (a). Box plot representing alpha diversity analysis (b, c) and PCoA representing beta diversity analysis (d, e) (Chao1) when humanized mice with DSS-induced colitis treated with SC-4 (Hum\_DSS\_SC-4), humanized mice gavage with SC-4 (Hum\_SC-4), Hum\_DSS, Hum (b,d), humanized mice treated with SC-4 with supplementation of Inulin (Hum\_Inulin\_SC-4), humanized mice with DSS-induced colitis treated with SC-4 with supplementation of Inulin (Hum\_DSS\_Inulin\_SC-4) and humanized mice with supplementation of Inulin (Hum\_Inulin) (c,e). Representative colon images from Hum, Hum\_DSS, Hum\_DSS\_SC-4, and Hum\_DSS\_Inulin\_SC-4 (f) and associated Violin plot (g) representing the length of the colon in cm. Statistical significance for (G) calculated using one-way ANOVA with Dunnett correction with absolute  $p$ -value represented on the graph. Bubble plot representing relative abundance in natural log scale at a species level resolution for SCFA producing bacteria (Similar to Figure 1(b)) from Hum, Hum\_DSS, Hum\_DSS\_SC-4, and Hum\_DSS\_Inulin\_SC-4 mice groups (h).

fact that SC-4 increased diversity, it also increased colon length, suggesting a higher rate of recovery for DSS-induced colitis (Figure 5(f,g)).

As fermentation of dietary fiber has been shown to promote the abundance of SCFA-producing species, we also examined whether the addition of dietary fiber could increase the abundance of SC-4 and provide better protection against colitis. To this end, the above set of experiments was repeated with and without inulin, a commonly used dietary fiber. Our analysis found that the addition of inulin increased the alpha diversity at a much higher rate (Figure 5(c)). When beta diversity was analyzed, we found that colonization of SC-4 with Inulin treated group clustered more toward control mice (Figure 5(e)). However, inulin and inulin with SC-4 administration in control mice had a different clustering, which was expected because of the effect of inulin on the microbiome (Figure 5(c)). This also proves that inulin alone is less efficient in increasing diversity compared to SC-4 supplementation. Further addition of inulin with SC-4 resulted in an increase in colon length compared to treatment with SC-4 alone (Figure 5(f,g)). Moreover, both SC-4 and Sc-4 with inulin treatment showed a decrease in diarrhea in mice as represented as fecal score 8 and 9 post-induction, respectively (Supplementary Figure S5I). Because we know that a stable microbial community is functionally redundant, we wanted to check whether DSS treatment showed this redundancy in humanized mice. To this end, we created a custom database of full-length 16S rDNA for the known SCFA-producing bacterial species, as shown in (Figure 1(a,b)) and checked their abundance in various treatments. This analysis showed a decrease in most of the highly abundant SCFA-producing bacteria upon DSS administration, while low-abundant bacterial species such as *Clostridium innocuum*, *Anaerostipes hadrus*, *Clostridium tyrobutyricum*, and *Hungatella hathewayi* increased in abundance (Figure 5(h)). Furthermore, in the case of SC-4 and SC-4 along with inulin treatment, the supplementation appeared to increase in the rest of the SCFA producers in the community (Figure 5(h)). Interestingly, in both treatments, we also found an increase in the abundance of *Akkermansia*

*muciniphila*, a known butyrate-producing species with known gut health-improving functions. This suggests that SC-4 administration might help regain SCFA production through interspecies interactions that boost other beneficial species.

We checked gene expression changes in the mouse colon upon colonization of humanized mice with the SC-4 consortium post euthanasia (day 23). As noticed in the case of GF mice, we did not observe any significant changes in inflammatory-related gene expression, further proving the nonpathogenic nature of the SC-4 consortium (Supplementary Figure S5j-l). An iNOS-dependent increase in colonic mucus has previously been demonstrated in colitis-induced rats. We observed a significant increase in iNOS expression when colitis-induced mice were treated with SC-4 or SC-4 supplemented with inulin (Figure 6(a-c)). We believe that SC-4 might be helping the mice to protect against more damage from colitis by increasing mucus production through the increase of iNOS. There was also a reduction in the expression of IL-6 compared to colitis recovered naturally. Myeloperoxidase (MPO) produces hypohalous acid to carry out its antimicrobial activity and is upregulated in colitis recovered naturally (Figure 6(a)). This might be due to the perturbation and community shift due to DSS-induced colitis, which increased the abundance of some pathogenic bacterial classes and, hence, the response. The same was downregulated when the mice were treated with SC-4 or SC-4 supplemented with inulin. This indirectly shows the ability of the consortium to transform the community into a healthy state. Histopathology of the colon sections showed several differences between BP-treated and untreated mice. Colitis-induced humanized mice (Supplementary Figure S6a) showed a phenotype similar to that of GF mice with colitis, whereas when treated with SC-4 or SC-4 supplemented with inulin (Figure 6(h), Supplementary Figure S6b) showed a phenotype similar to that of control mice. The pathology score was more than 0 for only humanized mice induced with colitis and not for any of the treatment (Figure 6(h)). PAS staining of the histology section confirmed our observation that iNOS associated goblet cell

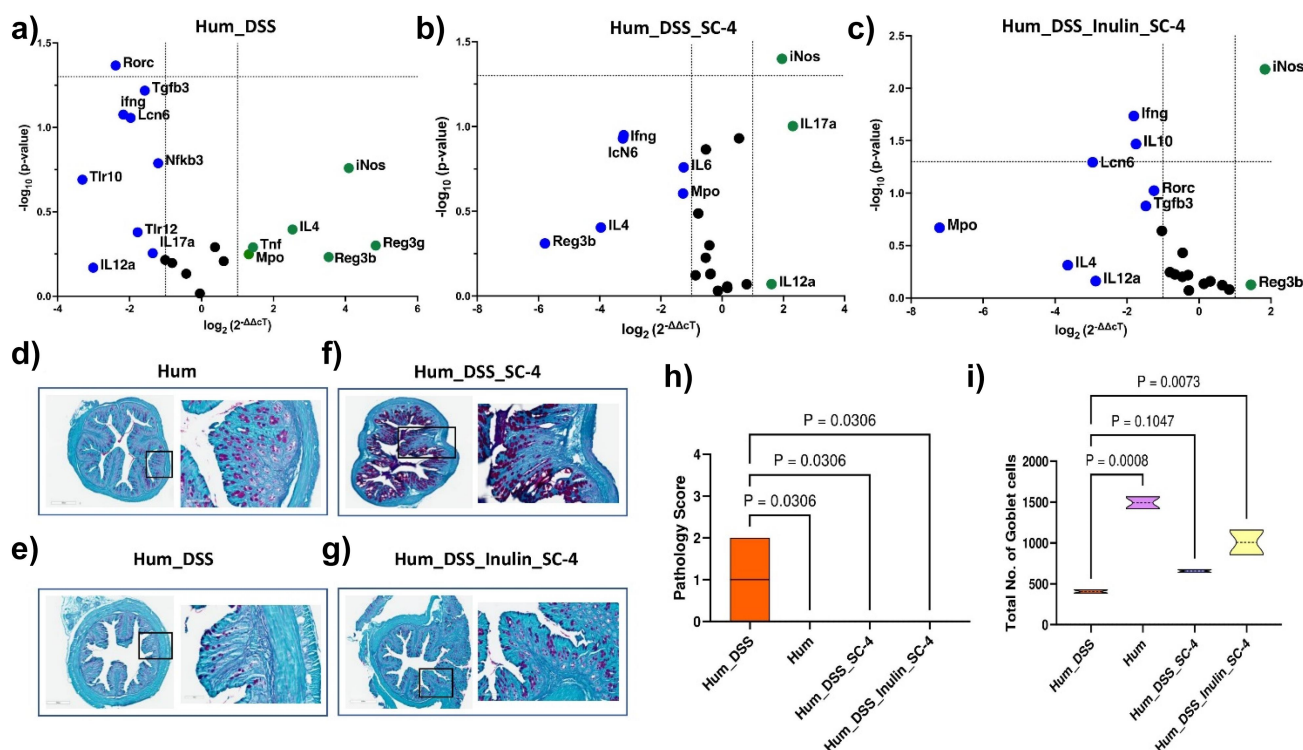


**Figure 6.** SC-4 colonization in humanized mice increases iNOS gene expression. RT-PCR gene expression for selected 25 immune-related genes of mice colon represented in volcano plot for humanized mice with DSS-induced colitis (Hum\_DSS) (a), humanized mice induced with colitis and treated with SC-4 (Hum\_DSS\_SC-4) (b), and humanized mice induced with colitis and treated with SC-4 and supplemented with Inulin (Hum\_DSS\_Inulin\_SC-4) compared to humanized mice control (Hum) (c). Green dots – overexpressed more than twofold change, green dots – overexpressed more than twofold compared to HUM control (dotted lines on the x-axis represent a twofold increase or decrease in expression and the y-axis represent a  $p$ -value cutoff of .05). Representative histopathological photograph showing the colon tissue cross-section after H&E staining for Hum (d), Hum\_DSS (e), Hum\_DSS\_SC-4 (f), Hum\_DSS\_Inulin\_SC-4 (g) mice groups. Pathology score calculated from the histopathological section of colon tissue cross section after H&E staining as mentioned in (Supplementary S6a,b) (h). Total number of goblet cells counted from the histopathological section of colon tissue cross section after PAS staining as mentioned in (D-G) (i). Statistical significance for H & I calculated using one-way ANOVA with Dunnett correction with absolute  $p$ -value represented on the graph.

increase. We saw an increase in the goblet cell number for both SC-4 and SC-4 and inulin treatment, but significant for Inulin and Sc-4 treatment only (Figures 6(d-i)). These results suggest that SC-4 with dietary fiber supplementation may help restore the dysbiotic microbiome.

## Discussion

In various biological systems such as terrestrial, aquatic, and animal gut microbiomes, a skewed distribution of species abundance is often observed. Within the healthy human gut microbiome, this phenomenon is particularly pronounced; while hundreds of species exist, only a few are present in high abundance, and the vast majority are found in low abundance.

Researchers refer to these low-abundant species as the “rare biosphere” of microbiomes.<sup>37</sup> This rarity can be visualized in a rank abundance plot, where the long tail represents these rare species after arranging them from high to low abundance. A challenge in studying this area is the lack of a universal cutoff for defining rarity. Most studies arbitrarily considered species with less than 0.1% abundance as rare or low abundant. Applying this threshold revealed that over 95% of the species in the human gut microbiome fit this category. Despite this prevalence, most microbiome research has concentrated on the functional role of high-abundance species, leaving the role of rare species relatively unexplored.

In this study, we investigated the role of four low-abundant gut bacterial species, *B. paravirosa*,

*C. comes*, *M. indica*, and *A. butyriciproducens*, on host health. These were chosen for their ability to produce short-chain fatty acids (SCFAs), a trait that we focused on because of SCFAs' importance in gut homeostasis. More specifically, these selected species were found to be low-abundant and possessed genes responsible for producing butyrate, a major SCFA with demonstrated positive effects on gut health. In our search for the abundance of these bacteria within a dataset of 598 metagenomes, which included samples from 50 subjects with Crohn's Disease (CD), 30 subjects with Ulcerative Colitis (UC) comprising 375 metagenomes, and 27 non-IBD subjects with a total of 365 metagenomes, we observed a decrease in the median abundance of all the bacteria in cases of UC or CD. However, this reduction was not statistically significant. Several studies have revealed that butyrate-producing genera such as *Alistipes*, *Barnesiella*, *Faecalibacterium*, *Oscillibacter*, *Agathobacter*, and *Ruminococcus* are depleted in patients with Inflammatory Bowel Disease (IBD).<sup>38</sup> Additionally, results from randomized controlled trials have shown that Fecal Microbiota Transplantation (FMT) can replenish lost diversity and ameliorate UC symptoms in affected patients.<sup>39,40</sup> However, the efficacy of defined bacteriotherapy or probiotic therapy in treating CD remains inconclusive.<sup>41,42</sup> This uncertainty might be attributed to the fact that most interventions have been carried out using high-abundant taxa such as Bifidobacteria and Lactobacilli.<sup>43</sup> The analysis was conducted using both germ-free and human microbiota-associated mouse models. We formed a synthetic consortium (SC-4) with the selected species and closely monitored their impact on host health, laying the groundwork for potential therapeutic applications targeting low-abundant, SCFA-producing gut bacteria.

Several traits common to high-abundance SCFA-producing species were also observed in the species examined in our study. Specifically, SC-4 colonized germ-free mice in large numbers and produced SCFAs (Figure 2). Importantly, the colonized mice displayed no signs of infection or pathology, indicating the safety of these strains. The primary effect of SC-4 colonization in germ-free mice was an increase in the expression of the MUC-1 and Muc2 genes and an increase in mucin

thickness in the colon. These results resemble those found in the treatment with sodium butyrate, which quadrupled ex vivo mucin synthesis in colonic biopsy specimens.<sup>44</sup> Similarly, treating human-polarized goblet cell lines with butyrate as an energy source augmented the expression of various MUC genes.<sup>45</sup> SC-4 colonization also conferred protection against DSS-induced colitis (Figure 3). Given that the protective efficacy observed in a germ-free animal model might not translate to a more complex microbiota environment, we tested SC-4's effectiveness using a human microbiota-associated mouse colitis model. Surprisingly, SC-4 not only cured the mice with colitis but also increased the microbiome diversity to a healthier state (Figures 5 and 6). *M. indica*, however, failed to colonize in this intricate setting. We noticed a similar increase in mucin thickness but did not observe any differences in MUC gene expression. Instead, a notable increase in iNos gene expression was detected, reminiscent of the iNos-mediated growth in colonic mucus observed in a colitis rat model.<sup>46</sup> We hypothesized that the same mechanism might apply to humanized mice for protection and cure. While the observed increase in iNOS expression associated with SC-4 treatment suggests a possible mechanism for enhanced mucus production, this hypothesis necessitates additional mechanistic studies for validation. There were no significant changes in the adaptive immune response in either germ-free or humanized mice.

The inability of SC-4 to show any visible differences in the adaptive immune profile and major signaling pathways compared to DSS-treated mice prompted us to ask whether the observed phenotype was associated with functional redundancy maintained by the humanized mouse gut community. We also found that the functionality of SCFA production was retained by the community, with an increase in some of the low-abundant SCFA producers after DSS treatment (Figure 5(h)). This is experimental proof for the insurance hypothesis being in existence for gut microbiome communities, similar to what has been reported for other biotic communities. This hypothesis extends from the broader theory that biodiversity sustains ecosystem stability by enabling alternative species to take over functional roles if others fail under altered conditions. Applied to the microbiome,

this diversity enables the microbial community to adapt to changes such as diet alterations, infections, or antibiotic treatments, continuing to provide vital functions, such as nutrient assimilation, immune system regulation, and resistance to pathogens.<sup>47</sup> This adaptive quality serves as an “insurance” against disruptions that could lead to dysfunction or illness. This phenomenon vanished when the system was introduced with SC-4. This poses important questions in microbiome research: Do prevalence studies identifying specific bacterial species presence in different physiological states correspond to this insurance species? Can we categorize a bacterial species to be associated with a disease by a mere increase in abundance in the gut community during the disease course? These questions must be answered before categorizing any bacteria that are positively associated with a disease. For instance, without considering this hypothesis, one can argue that the increased abundance of species in this study has a positive association with IBD.

Altogether, our findings enhance the fundamental understanding of the functions of low-abundant species and provide a proof-of-principle study for exploring these species as potential probiotic candidates. These results align with the biological insurance hypothesis within the gut microbial ecology.<sup>48</sup> Specifically, in the context of Inflammatory Bowel Disease (IBD), low-abundant species we tested may assume the roles of depleted high-abundant taxa such as *Alistipes*, *Barnesiella*, *Faecalibacterium*, *Oscillibacter*, *Agathobacter*, and *Ruminococcus*.<sup>38</sup> Further, population-level studies are required to confirm this possibility. The future research on the SC-4 bacterial consortium as a treatment for IBD will focus on understanding its ecological role on administration across diverse fecal microbiomes and how diet influences its therapeutic effectiveness. Key efforts will involve investigating the differential impacts of SC-4 and other low abundant SCFA producing microbiome members on metabolomic profiles in varied microbiome backgrounds, aiming to tailor treatments to individual gut ecologies. This approach promises to enhance the precision of microbiome-based therapies by incorporating patient-specific microbial compositions and dietary interactions, thereby optimizing the potential benefits of SC-4 in

managing IBD. Our present study paves the way for the exploration of low-abundant members in maintaining gut diversity and developing novel therapeutics against colitis.

## Materials and methods

### Animal experiments

Six-week-old C57BL/6 Germ-free (GF) mice were procured from Taconic Biosciences Inc. (New York, USA) and the Mayo Clinic (Rochester, USA). To negate any bias associated with gender differences, we ensured the inclusion of both male and female mice in our experiments, where feasible. All animals were subjected to a 12-hour light/dark cycle and provided with unlimited access to sterile drinking water and a standard chow diet. The protocols for all animal experiments were reviewed and approved by the South Dakota State University (SDSU) Institutional Animal Care and Use Committee (approval #19-014A).

### Bacteria culture and maintenance

The bacterial species utilized in our experiments were cultured and maintained using DSMZ modified PYG media, supplemented with L-cysteine as a reducing agent and resazurin as an oxygen indicator. The cultures were preserved at 37°C in an anaerobic chamber (Coy Lab Products Inc., MI, USA) filled with an atmospheric composition of 85% nitrogen, 10% carbon dioxide, and 5% hydrogen.

For *in-vitro* phenotypic assessment of butyrate production, overnight bacterial cultures were prepared in three distinct media conditions. These included Brain Heart Infusion broth and yeast extract-based media, with and without inulin as a complex carbohydrate supplement. The third medium used was DSMZ modified PYG medium. After 24 h of incubation in the anaerobic chamber, 100  $\mu$ L of the culture was combined with 500  $\mu$ L of 5% freshly prepared meta-phosphoric acid. This mixture was then thoroughly vortexed for 2 minutes and promptly stored at  $-80^{\circ}\text{C}$  for subsequent gas chromatography (GC) analysis, after which the optical density ( $\text{OD}_{600}$ ) of overnight grown cultures was adjusted to one, and aliquots were stored

in 12% DMSO at  $-80^{\circ}\text{C}$  until further use. On the day of inoculation, an equal volume of all four bacteria were resuspended and washed twice in the PYG medium. After centrifugation at 7000 RPM for 10 min, the bacterial pellets were reconstituted in PYG medium to get a 20 $\times$  concentrated bacterial suspension. About 100  $\mu\text{L}$ /mice of bacterial suspension were prepared and transferred to GF mice units in sterile, airtight 2 mL glass vials.

### **Mice experiments**

In our experiments involving gnotobiotic mice, we utilized a mixture of four butyrate-producing bacterial strains, referred to as the “Short-chain fatty acid producing consortium” (SC-4), for inoculation. A 200  $\mu\text{L}$  dose of this 20X concentrated bacterial mixture was administered to the treatment group via oral gavage. Each experimental group consisted of 4–6 mice, with an additional group of uninoculated mice serving as the germ-free control. Each mouse received two inoculations (once per day) and was subsequently allowed a colonization period ranging from a minimum of 14 days to a maximum of 28 days. At the conclusion of the colonization period, all mice were euthanized via cervical dislocation and samples were collected for subsequent analysis.

Colitis was chemically induced in germ-free (GF) mice following the protocol described by Wirtz et al.,<sup>49</sup> with slight modifications. Dextran sulfate sodium salt (30–50 KDa) from MP Biomedicals, USA, was added at a concentration of 1.5% to autoclaved drinking water. Mice had ad libitum access to DSS-infused water for 6 days, after which they were euthanized via cervical dislocation, and samples were subsequently collected for further analysis. On the fifth day, all animals displayed signs of rectal bleeding. One mouse in the GF group treated with DSS died on the sixth day of treatment. The onset of colitis was validated using a fecal occult test conducted on the third day.

In the case of human Fecal Microbiota Transplant (Hum) mice, both male and female 6-week-old mice received oral gavage of 200  $\mu\text{L}$  of the pooled fecal sample over three consecutive days, as described in our previous work.<sup>27</sup> After several generations of breeding, male and female

mice were exposed to 2.5% Dextran Sulfate Sodium (DSS) in their drinking water for 5 days to induce colitis. The mice were then switched to regular drinking water for another 3 days before being sacrificed in the Hum\_DSS group post 23 days. For the Hum\_DSS\_SC-4 and Hum\_DSS\_SC-4\_Inulin groups, mice were gavaged with 200  $\mu\text{L}$  of a 20X concentrated bacterial mixture for 2 days or the bacterial mix along with 1% inulin in their drinking water. In the Hum\_SC-4, Hum\_SC-4\_Inulin, and Hum\_Inulin groups, humanized mice were treated with the bacterial mix, bacterial mix along with inulin, or inulin only, and were then sacrificed after 23 days. Cecal and colon fecal samples were collected for 16S rRNA amplicon sequencing.

### **Fecal occult blood test**

The initiation of colitis was confirmed by an occult blood test using fecal samples. Whatman filter paper pre-treated with guaiac was used for this test. A thin smear of feces was applied to one side of a guaiac-coated Whatman filter paper. Subsequently, one or two drops of 3% hydrogen peroxide were carefully administered on the opposite side. A rapid transition to blue on Whatman paper was interpreted as a positive indication of the presence of blood in the sample.

### **Bacterial enumeration**

The total bacterial count in fecal samples collected at different time points was assessed to evaluate bacterial colonization. Anaerobically modified PYG medium (DSMZ medium) was used to enumerate the bacterial load, as this medium was found to support all four bacteria used in this study.

### **Genomic DNA extraction and targeted amplicon sequencing**

Genomic DNA was extracted from pure bacterial cultures using a DNeasy blood and tissue kit (Qiagen, Maryland, USA). We used the DNeasy power soil kit (Qiagen, Maryland, USA) to extract fecal samples and intestinal contents of the mice, according to the manufacturer’s instructions. The

16s rRNA gene sequencing was performed according to the standard Illumina protocol, where PCR amplicons targeting the V3-V4 region of the bacterial 16s rRNA gene were used for sequencing. Locus-specific primer pairs (16S Amplicon PCR Forward Primer = 5'CCTACGGGNGGCWGCAG and 16S Amplicon PCR Reverse Primer = 5' GACTACHVGGGTATCTAATCC) were attached to overhang adaptors (Forward overhang: 5' TCGTCGGCAGCGTCAGATGTGTATAAGAGACAG and Reverse overhang: 5' GTCTC GTGGGCTCGGAGATGTGTATAAGAGACAG) at the 5' end of the respective primer sequences (Illumina, Inc.) and used to amplify the region of interest.

The resulting amplicons were then cleaned of free primers and primer dimer species using AMPure XP beads (Beckman Coulter). Sequencing libraries were prepared using the Nextera XT library preparation kit (Illumina, Inc.). After indexing using a dual barcoding system according to the manufacturer's protocol and then normalizing to a concentration of 4 nM, the libraries were pooled into a single loading library. Sequencing was performed on an Illumina MiSeq platform using 2 × 300 bp paired-end read chemistry. Demultiplexed and adaptor-trimmed reads generated by Illumina analytical tools were used for further processing.

### **Bacterial community profiling**

Microbiota profiling from 16S sequencing was performed using Vsearch.<sup>50</sup> Merging and Quality filtering with a minimum cutoff length of 400 and maximum length of 500 were performed for the fastq files using the Vsearch tool. Singleton and chimeric reads (UCHIME) were removed. OTU selection was performed using VSEARCH abundance-based greedy clustering. OTUs were annotated using the SILVA reference database<sup>51</sup> or Custom database made from full-length 16s extracted from the whole genome of the four bacteria in the consortia. To create a custom database for the SCFA-producing bacterial consortium, we used the full-length 16s rRNA sequence obtained from SILVA/NCBI. The resulting OTU table was further processed for analysis. Alpha and beta diversity

calculations and plotting were performed using Microbiome Analyst with the default parameters.<sup>52</sup>

### **Bacterial species abundance mapping**

To assess the association of the four selected butyrate producers in IBD conditions, an abundance mapping at the strain level was performed using publicly available 1338 gut metagenome sequencing datasets collected from US individuals as a part of a longitudinal cohort research study by Lloyd et al.<sup>28</sup> For all metagenome reads, quality trimming and adapter clipping were performed using Trimmomatic.<sup>53</sup> Furthermore, the reads were aligned against the human genome to filter out human reads and assembled using Bowtie2 v2.3.2<sup>54</sup> and SAMtools.<sup>55</sup> The resulting contigs were classified taxonomically by k-mer analysis using Kraken2<sup>56</sup> with the Kraken 2 standard bacterial database built using Kraken-built. The subsequent estimation of species abundance was performed using the Kraken tools.<sup>57</sup>

### **Gas chromatography (GC) analysis for SCFAs**

Immediately before the GC analysis, the samples were thawed and vortexed for 2 min. The ethyl acetate (EA) extraction method described by Garcia-Villalba et al.<sup>58</sup> was used to detect SCFA. Briefly, the homogenized sample was centrifuged for 10 min at 17,949 × g. Each milliliter of supernatant was extracted with 1 mL of an organic solvent (EA) for 2 min and centrifuged for 10 min at 17,949 × g. A minimum of 200uL organic phase volume per sample was loaded in the Trace 1300 gas chromatogram (Thermo Fisher Scientific, USA).

### **Quantitative RT-PCR-based gene expression profiling**

To assess the localized response of host-microbe interactions following colonization of BP4 strains, 100 mg of tissue from the colon was sampled and snap-frozen in liquid nitrogen. The samples were then stored at -80°C until further processing. For RNA extraction, TRIzol® (Ambion, Life

Technologies, USA)-chloroform (Sigma-Aldrich, USA) was used. DNase treatment was performed using an RNase-Free DNase kit (Qiagen, Maryland, USA) according to the manufacturer's protocol to remove any contaminant genomic DNA. RNA quality and quantity were evaluated using a NanoDrop One (Thermo Scientific, USA) and stored at  $-80^{\circ}\text{C}$  until further use.

Complimentary DNA (cDNA) was prepared from 250 ng of total RNA using the First-Strand cDNA Synthesis Kit (New England BioLabs Inc., USA), according to the manufacturer's protocol. Host gene expression was assessed by qRT-PCR using an Rt2 profiler array (Qiagen, Maryland, USA) (Supplementary Table 1) or 25 defined immune-related genes (Supplementary Table 2). Reactions were prepared using the Power SYBR<sup>®</sup> Green PCR Master Mix (Applied Biosystems, USA). PCR was performed in an ABI7500 standard (Applied Biosystems, USA) RT-PCR machine under the following cycling conditions:  $95^{\circ}\text{C}$  for 10 min, 40 cycles of  $95^{\circ}\text{C}$  for 15 s, and  $60^{\circ}\text{C}$  for 1 min.

Raw cycle threshold ( $C_T$ ) values at a threshold of 0.15 were exported and then uploaded to the Qiagen data analysis center for further analysis. A  $C_T$  cutoff value of 30 was used for the analysis. The average geometric mean of the  $C_T$  values of two housekeeping genes, mouse beta-actin (Actb) and mouse glyceraldehyde phosphate dehydrogenase (Gapdh), were used for data normalization and  $\Delta C_T$  calculation. The fold change and fold regulation of gene expression were calculated using the  $\Delta\Delta C_T$  method.

### **Separation of lymphocytes from peripheral mouse blood**

Immediately after euthanasia, blood was collected via cardiac puncture, transferred to heparinized blood collection vials (BD Vacutainer), and gently mixed to prevent coagulation. SepMate TM PBMC isolation tubes (STEMCELL Technologies, Canada) were used to collect lymphocytes from blood. An equal volume of DPBS (Dulbecco's PBS) was added to the blood sample before transferring to SepMate TM tubes prefilled with 4.5 mL of Lymphoprep (STEMCELL Technologies, Canada) density gradient medium. The tubes were then centrifuged at  $1200 \times g$  for 10 min at room temperature. The top layer containing the

plasma and mononuclear cells (MNC) was transferred to a fresh 15 mL falcon tube by a single pour-off step. After washing twice with DPBS, the transferred MNCs were re-suspended in freezing media containing 10% DMSO and stored in liquid nitrogen until staining for flow cytometry.

### **Separation of lymphocytes from mouse spleen**

After removing the capsular layer in a sterile petri dish, the spleen was mechanically disrupted using sterile BP blades. The cell suspension in RPMI1640 media (Corning, USA) was filtered through a cell strainer (70  $\mu\text{M}$  Nylon mesh, Fisherbrand, USA) to make a single-cell suspension. Cells were washed once in RPMI 1640 (Corning, USA) and then treated with ammonium chloride solution (STEMCELL Technologies, Canada) at a 9:1 ratio in RPMI 1640 cell culture media for 7 min on ice to lyse RBCs. After lysing the RBCs, the cells were washed twice with RPMI 1640 medium, resuspended in freezing media containing 10% DMSO, and stored in liquid nitrogen until further use.

### **Flow cytometry analysis**

On average,  $10^5$ – $10^7$  cells were used for staining. A list of antibodies with fluorochrome was used, as in (Supplementary Table 3). Stained cells were fixed in IC fixation buffer (Thermo Fisher, USA) and run on an Attune NxT Flow cytometer (Thermo Fisher, USA). Raw files were exported to the FlowJo software for further analysis.

### **Histopathology sectioning and scoring**

Histological analysis was conducted on both the distal and proximal ends of the murine colon to evaluate the extent of tissue damage and the therapeutic effects of the interventions. Tissues were fixed in formalin, embedded in paraffin, and then sectioned at 10  $\mu\text{m}$  for staining. Hematoxylin and Eosin (H&E) staining was performed to assess general morphology and inflammation, while periodic acid-Schiff (PAS) staining was used to highlight goblet cell abundance and mucin production. A board-certified pathologist, blinded to the experimental conditions, evaluated the stained sections. The scoring system ranged from 0 (absent) to

4 (severe), based on the degree of inflammatory cell infiltration, epithelial damage, and mucosal architecture disruption observed. Scores of 1 indicated minimal changes, 2 mild changes, 3 moderate changes, and 4 severe pathologies. The scoring was independently performed for both the distal and proximal colon sections and reported based on inflammation.

### Statistical analysis

Statistical analyses were performed using GraphPad Prism 9 software (GraphPad Software, San Diego, CA, USA). Comparisons between groups were performed using either the Mann–Whitney *t*-test or *t*-test with Welch's correction unless mentioned in the figure legends. Differences were considered statistically significant at a *p* value of .05. A bubble plot was plotted in R using the ggplot package.

### Acknowledgments

Computations supporting this project were performed on High-Performance Computing systems managed by Research Computing Group, part of the Division of Technology and Security at South Dakota State University.

### Disclosure statement

No potential conflict of interest was reported by the author(s).

### Funding

This work was supported in part by USDA grant numbers [SD00H702-20, SD00R646-20] and the Walter R. Sitlington Endowment awarded to JS.

### Author contributions

AA, LA, AM, SG, and SM performed the experiments, VS performed the pathological analysis, JS and PK designed the study and provided resources. AA wrote the manuscript with input from other authors.

### Data availability statement

All 16s amplicon sequencing data generated from this project were deposited in the NCBI SRA database under BioProject

PRJNA1013066. Raw whole-genome sequence data for the strains used were obtained from a previously published study<sup>27</sup> under the BioProject PRJNA494608.

### Ethics statement

All animal procedures were approved by the Institutional Animal Care and Use Committee of South Dakota State University with the Prior approval of protocol 19-014A.

### References

1. Darwin C. On the origin of species by means of natural selection, or preservation of favoured races in the struggle for life. London: John Murray; 1859.
2. Preston FW. The commonness, and rarity, of species. *Ecology*. 1948;29(3):254–283. doi:10.2307/1930989.
3. Loftus M, Hassouneh SA-D, Yooseph S. Bacterial associations in the healthy human gut microbiome across populations. *Sci Rep*. 2021;11(1):2828. doi:10.1038/s41598-021-82449-0.
4. Forster SC, Kumar N, Anonye BO, Almeida A, Viciani E, Stares MD, Dunn M, Mkandawire TT, Zhu A, Shao Y, et al. A human gut bacterial genome and culture collection for improved metagenomic analyses. *Nat Biotechnol*. 2019;37(2):186–192. doi:10.1038/s41587-018-0009-7.
5. Porter NT, Luis AS, Martens EC. Bacteroides thetaiotaomicron. *Trends Microbiol*. 2018;26(11):966–967. doi:10.1016/j.tim.2018.08.005.
6. Lopez-Siles M, Duncan SH, Garcia-Gil LJ, Martinez-Medina M. Faecalibacterium prausnitzii: from microbiology to diagnostics and prognostics. *Isme J*. 2017;11(4):841–852. doi:10.1038/ismej.2016.176.
7. Conway T, Cohen PS, Conway T, Cohen P. Commensal and pathogenic Escherichia coli metabolism in the gut. *Microbiol Spectr*. 2015;3(3). doi:10.1128/microbiol.spec.MBP-0006-2014.
8. Pickard JM, Zeng MY, Caruso R, Núñez G. Gut microbiota: role in pathogen colonization, immune responses, and inflammatory disease. *Immunological Rev*. 2017;279(1):70–89. doi:10.1111/imr.12567.
9. May RM. Will a large complex system be stable? *Nature*. 1972;238(5364):413–414. doi:10.1038/238413a0.
10. MacArthur R. Fluctuations of animal populations and a measure of community stability. *ecology*. *Ecology*. 1955;36(3):533–536. doi:10.2307/1929601.
11. McCann KS. The diversity–stability debate. *Nature*. 2000;405(6783):228–233. doi:10.1038/35012234.
12. Ives AR, Carpenter SR. Stability and diversity of ecosystems. *Science*. 2007;317(5834):58–62. doi:10.1126/science.1133258.
13. Yachi S, Loreau M. Biodiversity and ecosystem productivity in a fluctuating environment: the insurance

- hypothesis. *Proc Natl Acad Sci USA*. 1999;96(4):1463–1468. doi:10.1073/pnas.96.4.1463.
14. Wittebolle L, Marzorati M, Clement L, Balloi A, Daffonchio D, Heylen K, De Vos P, Verstraete W, Boon N. Initial community evenness favours functionality under selective stress. *Nature*. 2009;458(7238):623–626. doi:10.1038/nature07840.
  15. Shade A, Gilbert JA. Temporal patterns of rarity provide a more complete view of microbial diversity. *Trends Microbiol*. 2015;23(6):335–340. doi:10.1016/j.tim.2015.01.007.
  16. Augeron C, Laboisse CL. Emergence of permanently differentiated cell clones in a human colonic cancer cell line in culture after treatment with sodium butyrate. *Cancer Res*. 1984;44(9):3961–3969.
  17. Barnard JA, Warwick G. Butyrate rapidly induces growth inhibition and differentiation in HT-29 cells. *Cell Growth Differ*. 1993;4(6):495–501.
  18. Kb A, Madhavan A, Tr R, Thomas S, Nisha P. Short chain fatty acids enriched fermentation metabolites of soluble dietary fibre from *Musa paradisiaca* drives HT29 colon cancer cells to apoptosis. *PLOS ONE*. 2019;14(5):e0216604. doi:10.1371/journal.pone.0216604.
  19. Kelly CJ, Zheng L, Campbell E, Saeedi B, Scholz C, Bayless A, Wilson K, Glover L, Kominsky D, Magnuson A, et al. Crosstalk between microbiota-derived short-chain fatty acids and intestinal epithelial HIF augments tissue barrier function. *Cell Host Microbe*. 2015;17(5):662–671. doi:10.1016/j.chom.2015.03.005.
  20. Cherbut C, Ferrier L, Rozé C, Anini Y, Blottière H, Lecannu G, Galmiche J-P. Short-chain fatty acids modify colonic motility through nerves and polypeptide YY release in the rat. *Am J Physiol-Gastrointestinal Liver Physiol*. 1998;275(6):G1415–G1422. doi:10.1152/ajpgi.1998.275.6.G1415.
  21. Matthews GM, Howarth GS, Butler RN. Short-chain fatty acids induce apoptosis in colon cancer cells associated with changes to intracellular redox state and glucose metabolism. *Chemotherapy*. 2012;58(2):102–109. doi:10.1159/000335672.
  22. Breuer RI, Soergel KH, Lashner BA, Christ ML, Hanauer SB, Vanagunas A, Harig JM, Keshavarzian A, Robinson M, Sellin JH, et al. Short chain fatty acid rectal irrigation for left-sided ulcerative colitis: a randomised, placebo controlled trial. *Gut*. 1997;40(4):485–491. doi:10.1136/gut.40.4.485.
  23. Hamer HM, Jonkers D, Venema K, Vanhoutvin S, Troost FJ, Brummer R-J. Review article: the role of butyrate on colonic function. *Aliment Pharmacol Ther*. 2008;27(2):104–119. doi:10.1111/j.1365-2036.2007.03562.x.
  24. Van Immerseel F, Ducatelle R, De Vos M, Boon N, Van De Wiele T, Verbeke K, Rutgeerts P, Sas B, Louis P, Flint HJ, et al. Butyric acid-producing anaerobic bacteria as a novel probiotic treatment approach for inflammatory bowel disease. *J Med Microbiol*. 2010;59(2):141–143. doi:10.1099/jmm.0.017541-0.
  25. Scheppach W, Sommer H, Kirchner T, Paganelli G-M, Bartram P, Christl S, Richter F, Dusel G, Kasper H. Effect of butyrate enemas on the colonic mucosa in distal ulcerative colitis. *Gastroenterology*. 1992;103(1):51–56. doi:10.1016/0016-5085(92)91094-K.
  26. Sokol H, Pigneur B, Watterlot L, Lakhdari O, Bermúdez-Humarán LG, Gratadoux J-J, Blugeon S, Bridonneau C, Furet J-P, Corthier G, et al. Faecalibacterium prausnitzii is an anti-inflammatory commensal bacterium identified by gut microbiota analysis of Crohn disease patients. *Proc Natl Acad Sci USA*. 2008;105(43):16731–16736. doi:10.1073/pnas.0804812105.
  27. Ghimire S, Roy C, Wongkuna S, Antony L, Maji A, Keena MC, Foley A, Scaria J. Identification of clostridioides difficile-inhibiting gut commensals using culturomics, phenotyping, and combinatorial community assembly. *Msystems*. 2020;5(1):e00620–19. doi:10.1128/mSystems.00620-19.
  28. Lloyd-Price J, Arze C, Ananthkrishnan AN, Schirmer M, Avila-Pacheco J, Poon TW, Andrews E, Ajami NJ, Bonham KS, Brislawn CJ, et al. Multi-omics of the gut microbial ecosystem in inflammatory bowel diseases. *Nature*. 2019;569(7758):655–662. doi:10.1038/s41586-019-1237-9.
  29. Fu X, Liu Z, Zhu C, Mou H, Kong Q. Nondigestible carbohydrates, butyrate, and butyrate-producing bacteria. *Crit Rev In Food Sci Nutr*. 2019;59(sup1):S130–S152. doi:10.1080/10408398.2018.1542587.
  30. Markowiak-Kopec P, Śliżewska K. The effect of probiotics on the production of short-chain fatty acids by human intestinal microbiome. *Nutrients*. 2020;12(4):1107. doi:10.3390/nu12041107.
  31. Nicholson K, Bjornevik K, Abu-Ali G, Chan J, Cortese M, Dedi B, Jeon M, Xavier R, Huttenhower C, Ascherio A, et al. The human gut microbiota in people with amyotrophic lateral sclerosis. *Amyotroph Lateral Scler Frontotemporal Degener*. 2021;22(3–4):186–194. doi:10.1080/21678421.2020.1828475.
  32. Louis P, Flint HJ. Formation of propionate and butyrate by the human colonic microbiota. *Environ Microbiol*. 2017;19(1):29–41. doi:10.1111/1462-2920.13589.
  33. Vital M, Howe AC, Tiedje JM, Moran MA. Revealing the bacterial butyrate synthesis pathways by analyzing (meta)genomic data. *MBio*. 2014;5(2):e00889. doi:10.1128/mBio.00889-14.
  34. Kostic AD, Xavier RJ, Gevers D. The microbiome in inflammatory bowel disease: current status and the future ahead. *Gastroenterology*. 2014;146(6):1489–1499. doi:10.1053/j.gastro.2014.02.009.
  35. Papadopoulos G, Kramer CD, Slocum CS, Weinberg EO, Hua N, Gudino CV, Hamilton JA, Genco CA. A mouse model for pathogen-induced chronic inflammation at local and systemic sites. *J Vis Exp*. 2014;2014(90):e51556. doi:10.3791/51556.

36. Ang Z, Xiong D, Wu M, Ding JL. FFAR2-FFAR3 receptor heteromerization modulates short-chain fatty acid sensing. *FASEB J.* 2018;32(1):289–303. doi:10.1096/fj.201700252RR.
37. Sogin ML, Morrison HG, Huber JA, Welch DM, Huse SM, Neal PR, Arrieta JM, Herndl GJ. Microbial diversity in the deep sea and the underexplored “rare biosphere”. *Proc Natl Acad Sci USA.* 2006;103(32):12115–12120. doi:10.1073/pnas.0605127103.
38. Willing BP, Dicksved J, Halfvarson J, Andersson AF, Lucio M, Zheng Z, Järnerot G, Tysk C, Jansson JK, Engstrand L, et al. A pyrosequencing study in twins shows that gastrointestinal microbial profiles vary with inflammatory bowel disease phenotypes. *Gastroenterology.* 2010;139(6):1844–1854.e1. doi:10.1053/j.gastro.2010.08.049.
39. Moayyedi P, Surette MG, Kim PT, Libertucci J, Wolfe M, Onischi C, Armstrong D, Marshall JK, Kassam Z, Reinisch W, et al. Fecal microbiota transplantation induces remission in patients with active ulcerative colitis in a randomized controlled trial. *Gastroenterology.* 2015;149(1):102–109.e6. doi:10.1053/j.gastro.2015.04.001.
40. Rossen NG, Fuentes S, van der Spek MJ, Tijssen JG, Hartman JHA, Duflou A, Löwenberg M, van den Brink GR, Mathus-Vliegen EMH, de Vos WM, et al. Findings from a randomized controlled trial of fecal transplantation for patients with ulcerative colitis. *Gastroenterology.* 2015;149(1):110–118.e4. doi:10.1053/j.gastro.2015.03.045.
41. Ledder O, Turner D. Antibiotics in IBD: still a role in the biological Era? *Inflamm Bowel Dis.* 2018;24(8):1676–1688. doi:10.1093/ibd/izy067.
42. Lewis JD, Ruemmele FM, Wu GD. Nutrition, gut microbiota and immunity: therapeutic targets for IBD. Concluding remarks. *Nestle Nutr Inst Workshop Ser.* 2014;79:161–162.
43. Turrone F, Ventura M, Buttó LF, Duranti S, O’Toole PW, Motherway MO, van Sinderen D. Molecular dialogue between the human gut microbiota and the host: a lactobacillus and Bifidobacterium perspective. *Cell Mol Life Sci.* 2014;71(2):183–203. doi:10.1007/s00018-013-1318-0.
44. Finnie IA, Dwarakanath AD, Taylor BA, Rhodes JM. Colonic mucin synthesis is increased by sodium butyrate. *Gut.* 1995;36(1):93–99. doi:10.1136/gut.36.1.93.
45. Gaudier E, Jarry A, Blottière HM, de Coppet P, Buisine MP, Aubert JP, Laboisse C, Cherbut C, Hoebler C. Butyrate specifically modulates MUC gene expression in intestinal epithelial goblet cells deprived of glucose. *Am J Physiol Gastrointest Liver Physiol.* 2004;287(6):G1168–74. doi:10.1152/ajpgi.00219.2004.
46. Schreiber O, Petersson J, Waldén T, Ahl D, Sandler S, Phillipson M, Holm L. iNOS-dependent increase in colonic mucus thickness in DSS-colitic rats. *PLoS One.* 2013;8(8):e71843. doi:10.1371/journal.pone.0071843.
47. Relman DA. The human microbiome: ecosystem resilience and health. *Nutr Rev.* 2012;70(Suppl 1):S2–9. doi:10.1111/j.1753-4887.2012.00489.x.
48. Loreau M, Naeem S, Inchausti P, Bengtsson J, Grime JP, Hector A, Hooper DU, Huston MA, Raffaelli D, Schmid B, et al. Biodiversity and ecosystem functioning: current knowledge and future challenges. *Science.* 2001;294(5543):804–808. doi:10.1126/science.1064088.
49. Wirtz S, Neufert C, Weigmann B, Neurath MF. Chemically induced mouse models of intestinal inflammation. *Nat Protoc.* 2007;2(3):541–546. doi:10.1038/nprot.2007.41.
50. Rognes T, Flouri T, Nichols B, Quince C, Mahé F. VSEARCH: a versatile open source tool for metagenomics. *PeerJ.* 2016;4:e2584. doi:10.7717/peerj.2584.
51. Quast C, Pruesse E, Yilmaz P, Gerken J, Schweer T, Yarza P, Peplies J, Glöckner FO. The SILVA ribosomal RNA gene database project: improved data processing and web-based tools. *Nucleic Acids Res.* 2013;41(Database issue):D590–6. doi:10.1093/nar/gks1219.
52. Dhariwal A, Chong J, Habib S, King IL, Agellon LB, Xia J. MicrobiomeAnalyst: a web-based tool for comprehensive statistical, visual and meta-analysis of microbiome data. *Nucleic Acids Res.* 2017;45(W1):W180–W188. doi:10.1093/nar/gkx295.
53. Bolger AM, Lohse M, Usadel B. Trimmomatic: a flexible trimmer for illumina sequence data. *Bioinformatics.* 2014;30(15):2114–2120. doi:10.1093/bioinformatics/btu170.
54. Langmead B, Salzberg SL. Fast gapped-read alignment with bowtie 2. *Nat Methods.* 2012;9(4):357–359. doi:10.1038/nmeth.1923.
55. Li H, Handsaker B, Wysoker A, Fennell T, Ruan J, Homer N, Marth G, Abecasis G, Durbin R. The sequence Alignment/Map format and SAMtools. *Bioinformatics.* 2009;25(16):2078–2079. doi:10.1093/bioinformatics/btp352.
56. Wood DE, Lu J, Langmead B. Improved metagenomic analysis with kraken 2. *Genome Biol.* 2019;20(1):257. doi:10.1186/s13059-019-1891-0.
57. Lu J, Rincon N, Wood DE, Breitwieser FP, Pockrandt C, Langmead B, Salzberg SL, Steinegger M. Metagenome analysis using the Kraken software suite. *Nat Protoc.* 2022;17:2815–2839. doi:10.1038/s41596-022-00738-y.
58. Garcia-Villalba R, Giménez-Bastida JA, García-Conesa MT, Tomás-Barberán FA, Carlos Espín J, Larrosa M. Alternative method for gas chromatography-mass spectrometry analysis of short-chain fatty acids in faecal samples. *J Sep Sci.* 2012;35(15):1906–1913. doi:10.1002/jssc.201101121.
59. Serban DE. Microbiota in inflammatory bowel disease pathogenesis and therapy: Is it all about diet? *Nutr Clin Pract. Nutr Clin Pract.* 2015;30(6):760–779. doi:10.1177/0884533615606898.